Five-level fuzzy logic direct torque control of double star synchronous machine

Elakhdar Benyoussef, Abdelkader Meroufel and Said Barkat

Abstract— This paper deals with the direct torque control of the salient-pole double star synchronous machine drive fed by two five-level diode-clamped inverters. This approach combines the well-known advantages of the multilevel inverter with those of a direct torque control. The proposed approach consist to replace the hysteresis controllers by one fuzzy controller and the output vector of the fuzzy controller is led to a multilevel switching table to decide which reference vector should be applied to control the two three-level inverters. Simulation results show some improvement regarding in the reduction of torque and flux ripples.

Keywords— Double Star Synchronous Machine, Multi-level Inverter, Direct Torque Control, Fuzzy Logic Control.

I. INTRODUCTION

FOR many years, electrical drives are founded on the traditional three-phase machines. However, when enhancing power capabilities of the drive is considered, multiphase machine drives are potentially recommended. In fact, multiphase drives are useful for large systems such as naval electric propulsions systems, locomotive traction and electrical vehicles applications [1].

Multiphase drives are often considered as a viable solution when reduction of the inverter per phase rating is required due to the high motor power. Furthermore, this category of drives has many advantages over conventional drives such as reducing the amplitude of torque pulsation, lowering the DC link current harmonics, higher reliability and decreasing the current stress of switching devices [2].

The multiphase machine used in electrical drive systems are in principle the same as their three-phase counterparts. These include asynchronous and synchronous multiphase machines. Synchronous multiphase machines may be with permanent magnet excitation or with field winding excitation [3], among these types of machines; the salient-pole double star synchronous machine (DSSM) is one of the most useful of multiphase machines. This kind of machine contains double stators displaced by 30 degrees; the rotor is similar to the rotor of a simple synchronous machine and it's excited by constant current source.

The feeding of this type of machine is generally assured by two two-level inverters. However, for the high power; multilevel inverters are often required. Since the advantages of multilevel inverters and multiphase machines complement each other, it appears to be logical to try to combine them by realizing a multilevel multiphase drive. Several topologies of multilevel inverters have been proposed in the technical literatures [4], [5]. The diode clamped inverter (DCI) represents one of the most interesting solutions, to increase voltage and power levels and to achieve high quality voltage waveforms [6]. This makes the DCI an attractive solution to high power drive systems.

In order to ensure an effective control of DSSM, several methods have been proposed [7]. Complexity and parameters sensitivity are the weakness of these methods. An alternative solution is the use of direct torque control (DTC) strategy [8]. Direct torque control method is characterized by its simple implementation and a fast dynamic response [9]. Considerable research effort is still being devoted to the elimination of its inherent disadvantages. One more significant disadvantage of conventional DTC is ripples, which exists in the torque and flux variables. Recently, several techniques have been developed [10], [11] to improve the torque performance. In this context, a FLDTC scheme applied on five-level DCI is proposed in this paper. Then, an appropriate voltage vector is selected. Simulations are then carried out to verify the performances of the proposed strategy. The simulation results obtained with the optimization in the rules number show good performances.

The remainder of this paper is structured as follows: in Section II the model of the DSSM is presented, a suitable transformation matrix is used to develop a simple dynamic model. The proposed five-level inverter is briefly presented in Section III. In Section IV, the DTC strategy is applied to get decoupled control of the flux and torque. In order to improve the static and dynamic control performance of the DSSM, the hysteresis controllers used in DTC are substituted by a fuzzy controller in Section V. Finally, the advantages of the proposed control system are shown by simulation involving 5 kW DSSM in Section VI.

II. MODELLING OF THE DOUBLE STAR SYNCHRONOUS MACHINE

In order to establish a model of DSSM, the usual assumptions are adopted: the MMF in air-gap has a sinusoidal repartition

E. Benyoussef is with the Intelligent Control & Electrical Power Systems laboratory, Djillali Liabes University, Sidi Bel Abbes, Algeria. (E-mail: lakhdarbenyoussef@yahoo.com).
A. Meroufel is with the Intelligent Control & Electrical Power Systems laboratory, Djillali Liabes University, Sidi Bel Abbes, Algeria. (E-mail: ameroufel@yahoo.fr).
S. Barkat is with the Faculty of Science and Engineering, Department of Electrical Engineering, M'sila University, Ichbilia Street, M'sila 28000, Algeria. (E-mail: Sa_Barkati@yahoo.fr).

and the saturation of magnetic circuit is neglected [7]. The stator and rotor voltages equations are given by:

$$v_s = R_s i_s + \frac{d}{dt}\phi_s \quad (1)$$

With:

v_s : Stator voltage vector.

i_s : Stator current vector.

ϕ_s : Stator flux vector.

The original six dimensional system of the machine can be decomposed into three orthogonal subspaces (α, β), (z_1, z_2) and (z_3, z_4) [3], using the following transformation.

$$\begin{bmatrix} X_\alpha & X_\beta & X_{z1} & X_{z2} & X_{z3} & X_{z4} \end{bmatrix}^T = [A][X_s] \quad (2)$$

With:

$$[X_s] = \begin{bmatrix} X_{s1} & X_{s2} \end{bmatrix}^T = \begin{bmatrix} X_{sa1} & X_{sb1} & X_{sc1} & X_{sa2} & X_{sb2} & X_{sc2} \end{bmatrix}^T$$

Where: X_s represents stator currents (i_s), stator flux (ϕ_s), and stator voltages (v_s).

The matrix A is given by:

$$[A] = \frac{1}{\sqrt{3}} \begin{bmatrix} \cos(0) & \cos\left(\frac{2\pi}{3}\right) & \cos\left(\frac{4\pi}{3}\right) & \cos(\gamma) & \cos\left(\frac{2\pi}{3}+\gamma\right) & \cos\left(\frac{4\pi}{3}+\gamma\right) \\ \sin(0) & \sin\left(\frac{2\pi}{3}\right) & \sin\left(\frac{4\pi}{3}\right) & \sin(\gamma) & \sin\left(\frac{2\pi}{3}+\gamma\right) & \sin\left(\frac{4\pi}{3}+\gamma\right) \\ \cos(0) & \cos\left(\frac{4\pi}{3}\right) & \cos\left(\frac{2\pi}{3}\right) & \cos(\pi-\gamma) & \cos\left(\frac{\pi}{3}-\gamma\right) & \cos\left(\frac{5\pi}{3}-\gamma\right) \\ \sin(0) & \sin\left(\frac{4\pi}{3}\right) & \sin\left(\frac{2\pi}{3}\right) & \sin(\pi-\gamma) & \sin\left(\frac{\pi}{3}-\gamma\right) & \sin\left(\frac{5\pi}{3}-\gamma\right) \\ 1 & 1 & 1 & 0 & 0 & 0 \\ 0 & 0 & 0 & 1 & 1 & 1 \end{bmatrix} \quad (3)$$

To express the stator and rotor equations in the same stationary reference frame, the following rotation transformation is adopted

$$P(\theta) = \begin{pmatrix} \cos(\theta) & \sin(\theta) \\ -\sin(\theta) & \cos(\theta) \end{pmatrix} \quad (4)$$

With this transformation, the components of the α-β plane can be expressed in the d-q plane as:

The electrical equations

$$\begin{cases} v_d = R_s i_d + \dfrac{d\phi_d}{dt} - \omega\phi_q \\ v_q = R_s i_q + \dfrac{d\phi_q}{dt} + \omega\phi_d \\ v_f = R_f i_f + \dfrac{d\phi_f}{dt} \end{cases} \quad (5)$$

With:

v_d, v_q : *d-q* axis stator voltages.

i_d, i_q : *d-q* axis stator currents.

ϕ_d, ϕ_q : *d-q* axis stator flux.

v_f, i_f : DC voltage and current of rotor excitation.

ϕ_f : Flux of rotor excitation.

R_s : Stator resistance.

R_f : Rotor resistance.

ω : Rotating speed of rotor flux linkage.

The flux equations

$$\begin{cases} \phi_d = L_d i_d + M_{fd} i_f \\ \phi_q = L_q i_q \\ \phi_f = L_f i_f + M_{fd} i_d \end{cases} \quad (6)$$

With:

L_d, L_q : *d-q* stator inductance.

L_f : *d* axis rotor inductance.

M_{fd} : Mutual inductance between *d* axis for each stator and rotor.

The mechanical equation

$$J\frac{d\Omega}{dt} = T_{em} - T_L - f_r\Omega \quad (7)$$

With:

T_{em}, T_L : Electromagnetic and load torque.

Ω : Rotor speed.

J : Moment inertia.

f_r : Friction coefficient.

The electromagnetic torque equation is given by:

$$T_{em} = p(\phi_d i_q - \phi_q i_d) \quad (8)$$

With: p is the pole pair number.

III. Structure of Five-Level Inverter

The main circuit of the five-level DCI is shown in figure 1. The DC bus capacitor is split into four, providing a three neutral-point. Each arm of the inverter is made up of eight IGBTs (Insulated Gate Bipolar Transistor) devices, and six clamping diodes connected to the neutral-point. The advantage of the inverter is that circuit topology is simple, the output is connected with the machine directly, no transformer needed. The voltage stress of switching device is only quarter of the DC bus voltage; it is easy to extend the capacity of inverter.

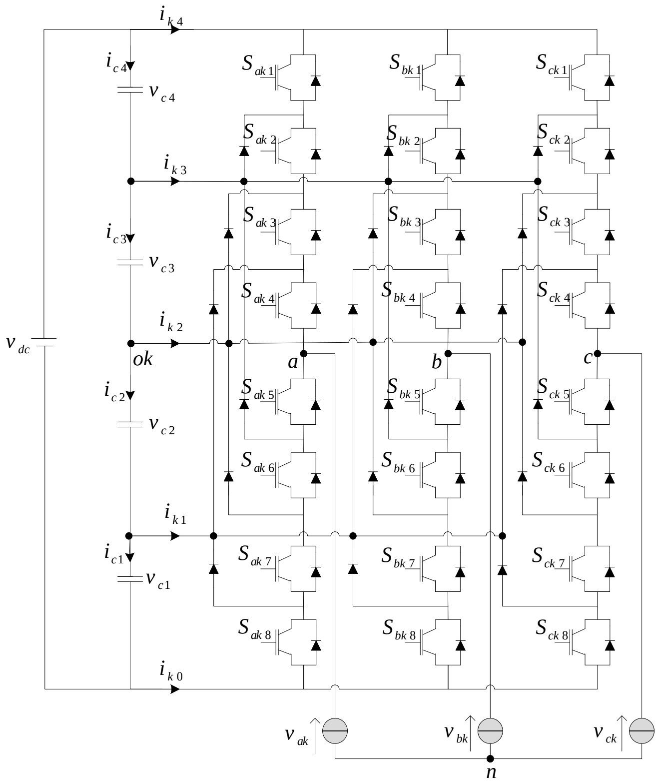

Fig. 1 Structure of five-level diode-clamped inverter (*k=1* for first inverter and *k=2* for second inverter).

Since five kinds of switching states exist in each phase, a five-level inverter has 125 switching states and there are 61 effective vectors (figure 2).

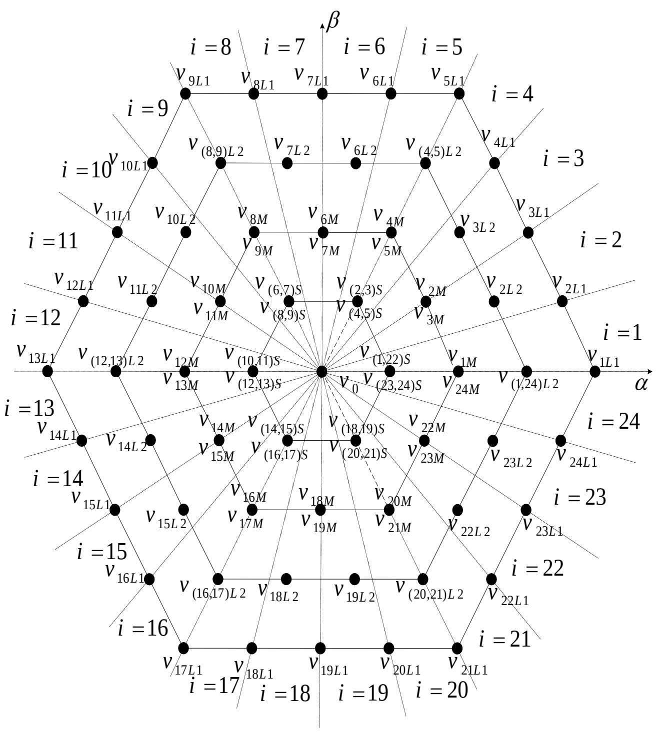

Fig. 2 Space voltage vectors for a five-level DCI.

For each switching device S_{xki} ($k=1, 2$, $i= 1\ldots 8$, $x=$a, b *or* c), a Boolean function F_{xki} is defined by:

$$F_{xki} = \begin{cases} 1 & if \quad S_{xki} \quad is \quad ON \\ 0 & if \quad S_{xki} \quad is \quad OFF \end{cases} \tag{9}$$

The complementarities between upper and lower switching devices of each leg impose the following equations:

$$F_{xki} = 1 - F_{xk(i-4)} \tag{10}$$

For each leg of the inverter, five connection functions are defined as follow:

$$\begin{cases} F_{Cxk1} = F_{xk1}F_{xk2}F_{xk3}F_{xk4} \\ F_{Cxk2} = F_{xk2}F_{xk3}F_{xk4}F_{xk5} \\ F_{Cxk3} = F_{xk3}F_{xk4}F_{xk5}F_{xk6} \\ F_{Cxk4} = F_{xk4}F_{xk5}F_{xk6}F_{xk7} \\ F_{Cxk5} = F_{xk5}F_{xk6}F_{xk7}F_{xk8} \end{cases} \tag{11}$$

The phase voltages v_{ak}, v_{bk}, v_{ck} can be written as:

$$\begin{pmatrix} v_{ak} \\ v_{bk} \\ v_{ck} \end{pmatrix} = \begin{pmatrix} F_{Cak1} & F_{Cak2} & F_{Cak3} & F_{Cak4} & F_{Cak5} \\ F_{Cbk1} & F_{Cbk2} & F_{Cbk3} & F_{Cbk4} & F_{Cbk5} \\ F_{Cck1} & F_{Cck2} & F_{Cck3} & F_{Cck4} & F_{Cck5} \end{pmatrix} \begin{pmatrix} v_{dc}/2 \\ v_{dc}/4 \\ 0 \\ -v_{dc}/4 \\ -v_{dc}/2 \end{pmatrix} \tag{12}$$

IV. Direct Torque Control Strategy

The well-known DTC strategy is based on flux and torque control using hysteresis comparators. These controllers use the estimated errors of the control variables at each sampling time of operation. The considered flux and torque controllers ensure the separate control of these two variables, as for the DC drives. When the level of torque or stator flux passes to the high or low hysteresis limit, a suitable voltage vector is applied to bring back each variable in its corresponding band [8].

The stator voltage estimator is given by:

$$\begin{bmatrix} \hat{v}_{\alpha} \\ \hat{v}_{\beta} \end{bmatrix} = \begin{bmatrix} A \end{bmatrix} \begin{bmatrix} \hat{v}_{s1} \\ \hat{v}_{s2} \end{bmatrix} \tag{13}$$

Where $\hat{v}_{s1}$ and $\hat{v}_{s2}$ are computed using Eq (12).

The stator flux vector components and its amplitude can be evaluated from the estimated stator voltage equation as follows

$$\begin{cases} \hat{\phi}_\alpha = \int_0^t (\hat{v}_\alpha - R_s i_\alpha) d\tau + \hat{\phi}_\alpha(0) \\ \hat{\phi}_\beta = \int_0^t (\hat{v}_\beta - R_s i_\beta) d\tau + \hat{\phi}_\beta(0) \\ \left|\hat{\phi}_s\right| = \sqrt{\hat{\phi}_\alpha^2 + \hat{\phi}_\beta^2} \end{cases} \quad (14)$$

The stator flux angle is calculated by:

$$\hat{\theta}_s = \tan 2^{-1}\left(\frac{\hat{\phi}_\beta}{\hat{\phi}_\alpha}\right) \quad (15)$$

The electromagnetic torque can be estimated by:

$$\hat{T}_{em} = p(\hat{\phi}_\alpha i_\beta - \hat{\phi}_\beta i_\alpha) \quad (16)$$

Tables 1 and 2 present the output voltage vectors which are selected to change the torque angle.

Table 1. Switching table used in the DTC of first star for the

Φ	τ	$Zone(i)$	Φ	τ	$Zone(i)$	Φ	τ	$Zone(i)$
	4	$v_{(i+4)L1}$		4	$v_{(i+6)L1}$		4	$v_{(i+8)L1}$
	3	$v_{(i+4)L2}$		3	$v_{(i+6)L2}$		3	$v_{(i+8)L2}$
	2	$v_{(i+4)M}$		2	$v_{(i+6)M}$		2	$v_{(i+8)M}$
	1	$v_{(i+4)S}$		1	$v_{(i+6)S}$		1	$v_{(i+8)S}$
1	0	v_0	0	0	v_0	−1	0	v_0
	−1	$v_{(i+20)S}$		−1	$v_{(i+18)S}$		−1	$v_{(i+16)S}$
	−2	$v_{(i+20)M}$		−2	$v_{(i+18)M}$		−2	$v_{(i+16)M}$
	−3	$v_{(i+20)L2}$		−3	$v_{(i+18)L2}$		−3	$v_{(i+16)L2}$
	−4	$v_{(i+20)L1}$		−4	$v_{(i+18)L1}$		−4	$v_{(i+16)L1}$

Table 2. Switching table used in the DTC of second star for the DSSM

Φ	τ	$Zone(i)$	Φ	τ	$Zone(i)$	Φ	τ	$Zone(i)$
	4	$v_{(i+2)L1}$		4	$v_{(i+4)L1}$		4	$v_{(i+6)L1}$
	3	$v_{(i+2)L2}$		3	$v_{(i+4)L2}$		3	$v_{(i+6)L2}$
	2	$v_{(i+2)M}$		2	$v_{(i+4)M}$		2	$v_{(i+6)M}$
	1	$v_{(i+2)S}$		1	$v_{(i+4)S}$		1	$v_{(i+6)S}$
1	0	v_0	0	0	v_0	−1	0	v_0
	−1	$v_{(i+18)S}$		−1	$v_{(i+16)S}$		−1	$v_{(i+14)S}$
	−2	$v_{(i+18)M}$		−2	$v_{(i+16)M}$		−2	$v_{(i+14)M}$
	−3	$v_{(i+18)L2}$		−3	$v_{(i+16)L2}$		−3	$v_{(i+14)L2}$
	−4	$v_{(i+18)L1}$		−4	$v_{(i+16)L1}$		−4	$v_{(i+14)L1}$

The DTC block diagram of DSSM supplied by five-level DCI in each star is represented by figure 3.

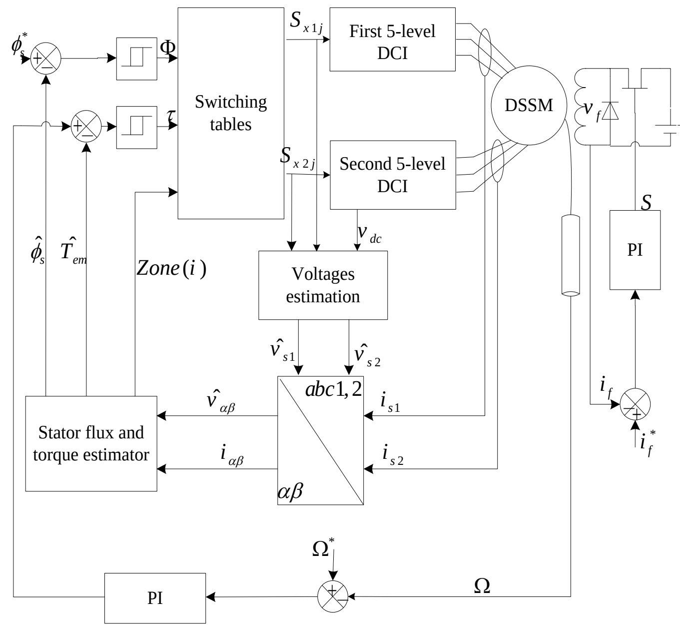

Fig. 3 Five-level DTC scheme for DSSM.

V. Fuzzy Logic Direct Torque Control Strategy

The principle of fuzzy logic direct torque control is similar to traditional DTC. However, the hysteresis controllers are replaced by fuzzy controller and the output vector of the fuzzy controller is led to a switching table to decide which vector should be applied. This method based on fuzzy classification has the advantage of simplicity and easy implementation [7, 9].

Figure 4 gives the membership functions for input variables E_T, E_ϕ and $\hat{\theta}_s$. For this purpose it is assumed that the stator flux linkage space vector can be located in any of twelve sectors presented in figure 4.

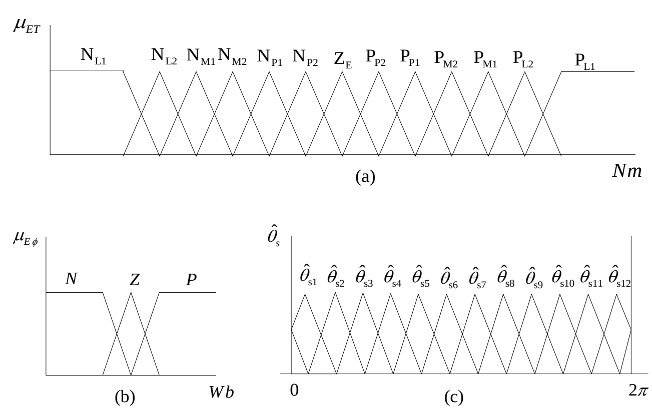

Fig. 4 Membership functions of input variables: a). Torque error, b). Stator flux error, c). Stator flux angle.

The fuzzy control rule base, developed using Mamdani's method, is shown in tables 3 and 4.

Table 3. Rules of fuzzy control for first star.

$\hat{\theta}_{s1}$

E_T \ E_ϕ	P	Z	N
$PL1$	v_{5L1}	v_{6M}	v_{9L1}
$PL2$	v_{6L1}	v_{6M}	v_{10L1}
$PM1$	v_{7L1}	v_{6M}	v_{11L1}
$PM2$	v_{4L2}	v_{2S}	v_{8L2}
$PS1$	v_{3L2}	v_{2S}	v_{7L2}
$PS2$	v_{4M}	v_{2S}	v_{8M}
ZE	v_0	v_0	v_0
$NL1$	v_{20M}	v_0	v_{16M}
$NL2$	v_{22L2}	v_{14S}	v_{18L2}
$NM1$	v_{20L2}	v_{18M}	v_{16L2}
$NM2$	v_{23L1}	v_{16M}	v_{19L1}
$NS1$	v_{22L1}	v_{18L2}	v_{18L1}
$NS2$	v_{21L1}	v_{16L2}	v_{17L1}

$\hat{\theta}_{s2}$

E_T \ E_ϕ	P	Z	N
$PL1$	v_{5L1}	v_{6M}	v_{9L1}
$PL2$	v_{8L1}	v_{6M}	v_{12L1}
$PM1$	v_{7L1}	v_{6M}	v_{11L1}
$PM2$	v_{4L2}	v_{2S}	v_{8L2}
$PS1$	v_{6L2}	v_{2S}	v_{10L2}
$PS2$	v_{4M}	v_{2S}	v_{8M}
ZE	v_0	v_0	v_0
$NL1$	v_{20M}	v_0	v_{16M}
$NL2$	v_{23L2}	v_{14S}	v_{19L2}
$NM1$	v_{20L2}	v_{18M}	v_{16L2}
$NM2$	v_{23L1}	v_{16M}	v_{19L1}
$NS1$	v_{24L1}	v_{19L2}	v_{20L1}
$NS2$	v_{21L1}	v_{16L2}	v_{17L1}

$\hat{\theta}_{s3}$

E_T \ E_ϕ	P	Z	N
$PL1$	v_{9L1}	v_{10M}	v_{13L1}
$PL2$	v_{10L1}	v_{10M}	v_{14L1}
$PM1$	v_{11L1}	v_{10M}	v_{15L1}
$PM2$	v_{8L2}	v_{6S}	v_{12L2}
$PS1$	v_{7L2}	v_{6S}	v_{11L2}
$PS2$	v_{8M}	v_{6S}	v_{12M}
ZE	v_0	v_0	v_0
$NL1$	v_{1M}	v_0	v_{20M}
$NL2$	v_{2L2}	v_{18S}	v_{22L2}
$NM1$	v_{1L2}	v_{22M}	v_{20L2}
$NM2$	v_{3L1}	v_{20M}	v_{23L1}
$NS1$	v_{2L1}	v_{22L2}	v_{22L1}
$NS2$	v_{1L1}	v_{20L2}	v_{21L1}

$\hat{\theta}_{s4}$

E_T \ E_ϕ	P	Z	N
$PL1$	v_{9L1}	v_{10M}	v_{13L1}
$PL2$	v_{12L1}	v_{10M}	v_{16L1}
$PM1$	v_{11L1}	v_{10M}	v_{15L1}
$PM2$	v_{8L2}	v_{6S}	v_{12L2}
$PS1$	v_{10L2}	v_{6S}	v_{14L2}
$PS2$	v_{8M}	v_{6S}	v_{12M}
ZE	v_0	v_0	v_0
$NL1$	v_{1M}	v_0	v_{20M}
$NL2$	v_{2L2}	v_{18S}	v_{23L2}
$NM1$	v_{1L2}	v_{22M}	v_{20L2}
$NM2$	v_{3L1}	v_{20M}	v_{23L1}
$NS1$	v_{4L1}	v_{23L2}	v_{24L1}
$NS2$	v_{1L1}	v_{20L2}	v_{21L1}

$\hat{\theta}_{s5}$

E_T \ E_ϕ	P	Z	N
$PL1$	V_{13L1}	v_{14M}	v_{17L1}
$PL2$	v_{14L1}	v_{14M}	v_{18L1}
$PM1$	v_{15L1}	v_{14M}	v_{19L1}
$PM2$	v_{12L2}	v_{10S}	v_{16L2}
$PS1$	v_{11L2}	v_{10S}	v_{15L2}
$PS2$	v_{12M}	v_{10S}	v_{16M}
ZE	v_0	v_0	v_0
$NL1$	v_{4M}	v_0	v_{1M}
$NL2$	v_{6L2}	v_{1S}	v_{2L2}
$NM1$	v_{4L2}	v_{2M}	v_{1L2}
$NM2$	v_{7L1}	v_{1M}	v_{3L1}
$NS1$	v_{6L1}	v_{2L2}	v_{2L1}
$NS2$	v_{5L1}	v_{1L2}	v_{1L1}

$\hat{\theta}_{s6}$

E_T \ E_ϕ	P	Z	N
$PL1$	V_{13L1}	v_{14M}	v_{17L1}
$PL2$	v_{16L1}	v_{14M}	v_{20L1}
$PM1$	v_{15L1}	v_{14M}	v_{19L1}
$PM2$	v_{12L2}	v_{10S}	v_{16L2}
$PS1$	v_{14L2}	v_{10S}	v_{18L2}
$PS2$	v_{12M}	v_{10S}	v_{16M}
ZE	v_0	v_0	v_0
$NL1$	v_{4M}	v_0	v_{1M}
$NL2$	v_{7L2}	v_{1S}	v_{3L2}
$NM1$	v_{4L2}	v_{2M}	v_{1L2}
$NM2$	v_{7L1}	v_{1M}	v_{3L1}
$NS1$	v_{8L1}	v_{3L2}	v_{4L1}
$NS2$	v_{5L1}	v_{1L2}	v_{1L1}

$\hat{\theta}_{s7}$

E_T \ E_ϕ	P	Z	N
$PL1$	V_{17L1}	v_{18M}	v_{21L1}
$PL2$	v_{18L1}	v_{18M}	v_{22L1}
$PM1$	v_{19L1}	v_{18M}	v_{23L1}
$PM2$	v_{16L2}	v_{14S}	v_{20L2}
$PS1$	v_{15L2}	v_{14S}	v_{19L2}
$PS2$	v_{16M}	v_{14S}	v_{20M}
ZE	v_0	v_0	v_0
$NL1$	v_{8M}	v_0	v_{4M}
$NL2$	v_{10L2}	v_{2S}	v_{6L2}
$NM1$	v_{8L2}	v_{6M}	v_{4L2}
$NM2$	v_{11L1}	v_{4M}	v_{7L1}
$NS1$	v_{10L1}	v_{6L2}	v_{6L1}
$NS2$	v_{9L1}	v_{4L2}	v_{5L1}

$\hat{\theta}_{s8}$

E_T \ E_ϕ	P	Z	N
$PL1$	V_{17L1}	v_{18M}	v_{21L1}
$PL2$	v_{20L1}	v_{18M}	v_{24L1}
$PM1$	v_{19L1}	v_{18M}	v_{23L1}
$PM2$	v_{16L2}	v_{14S}	v_{20L2}
$PS1$	v_{18L2}	v_{14S}	v_{22L2}
$PS2$	v_{16M}	v_{14S}	v_{20M}
ZE	v_0	v_0	v_0
$NL1$	v_{8M}	v_0	v_{4M}
$NL2$	v_{11L2}	v_{2S}	v_{7L2}
$NM1$	v_{8L2}	v_{6M}	v_{4L2}
$NM2$	v_{11L1}	v_{4M}	v_{7L1}
$NS1$	v_{12L1}	v_{7L2}	v_{8L1}
$NS2$	v_{9L1}	v_{4L2}	v_{5L1}

$\hat{\theta}_{s9}$

E_T \ E_ϕ	P	Z	N
$PL1$	v_{21L1}	v_{22M}	v_{1L1}
$PL2$	v_{22L1}	v_{22M}	v_{2L1}
$PM1$	v_{23L1}	v_{22M}	v_{3L1}
$PM2$	v_{20L2}	v_{18S}	v_{1L2}
$PS1$	v_{19L2}	v_{18S}	v_{23L2}
$PS2$	v_{20M}	v_{18S}	v_{1M}
ZE	v_0	v_0	v_0
$NL1$	v_{12M}	v_0	v_{8M}
$NL2$	v_{14L2}	v_{6S}	v_{10L2}
$NM1$	v_{12L2}	v_{10M}	v_{8L2}
$NM2$	v_{15L1}	v_{8M}	v_{11L1}
$NS1$	v_{14L1}	v_{10L2}	v_{10L1}
$NS2$	v_{13L1}	v_{8L2}	v_{9L1}

$\hat{\theta}_{s10}$

E_T \ E_ϕ	P	Z	N
$PL1$	v_{21L1}	v_{22M}	v_{1L1}
$PL2$	v_{24L1}	v_{22M}	v_{3L1}
$PM1$	v_{23L1}	v_{22M}	v_{4L1}
$PM2$	v_{20L2}	v_{18S}	v_{1L2}
$PS1$	v_{22L2}	v_{18S}	v_{2L2}
$PS2$	v_{20M}	v_{18S}	v_{1M}
ZE	v_0	v_0	v_0
$NL1$	v_{12M}	v_0	v_{8M}
$NL2$	v_{15L2}	v_{6S}	v_{11L2}
$NM1$	v_{12L2}	v_{10M}	v_{8L2}
$NM2$	v_{15L1}	v_{8M}	v_{11L1}
$NS1$	v_{16L1}	v_{11L2}	v_{12L1}
$NS2$	v_{13L1}	v_{8L2}	v_{9L1}

$\hat{\theta}_{s11}$

E_T \ E_ϕ	P	Z	N
$PL1$	v_{1L1}	v_{2M}	v_{5L1}
$PL2$	v_{2L1}	v_{2M}	v_{6L1}
$PM1$	v_{3L1}	v_{2M}	v_{7L1}
$PM2$	v_{1L2}	v_{1S}	v_{4L2}
$PS1$	v_{23L2}	v_{1S}	v_{3L2}
$PS2$	v_{1M}	v_{1S}	v_{4M}
ZE	v_0	v_0	v_0
$NL1$	v_{16M}	v_0	v_{12M}
$NL2$	v_{18L2}	v_{10S}	v_{14L2}
$NM1$	v_{16L2}	v_{14M}	v_{12L2}
$NM2$	v_{19L1}	v_{12M}	v_{15L1}
$NS1$	v_{18L1}	v_{14L2}	v_{14L1}
$NS2$	v_{17L1}	v_{12L2}	v_{13L1}

$\hat{\theta}_{s12}$

E_T \ E_ϕ	P	Z	N
$PL1$	v_{1L1}	v_{2M}	v_{5L1}
$PL2$	v_{4L1}	v_{2M}	v_{8L1}
$PM1$	v_{3L1}	v_{2M}	v_{7L1}
$PM2$	v_{1L2}	v_{1S}	v_{4L2}
$PS1$	v_{2L2}	v_{1S}	v_{6L2}
$PS2$	v_{1M}	v_{1S}	v_{4M}
ZE	v_0	v_0	v_0
$NL1$	v_{16M}	v_0	v_{12M}
$NL2$	v_{19L2}	v_{10S}	v_{14L2}
$NM1$	v_{16L2}	v_{14M}	v_{12L2}
$NM2$	v_{19L1}	v_{12M}	v_{15L1}
$NS1$	v_{20L1}	v_{15L2}	v_{14L1}
$NS2$	v_{17L1}	v_{12L2}	v_{13L1}

Table 4. Rules of fuzzy control for second star.

$Star1$	$\hat{\theta}_{s1}$	$\hat{\theta}_{s2}$	$\hat{\theta}_{s3}$	$\hat{\theta}_{s4}$	$\hat{\theta}_{s5}$	$\hat{\theta}_{s6}$	$\hat{\theta}_{s7}$	$\hat{\theta}_{s8}$	$\hat{\theta}_{s9}$	$\hat{\theta}_{s10}$	$\hat{\theta}_{s11}$	$\hat{\theta}_{s12}$
$Star2$	$\hat{\theta}_{s12}$	$\hat{\theta}_{s1}$	$\hat{\theta}_{s2}$	$\hat{\theta}_{s3}$	$\hat{\theta}_{s4}$	$\hat{\theta}_{s5}$	$\hat{\theta}_{s6}$	$\hat{\theta}_{s7}$	$\hat{\theta}_{s8}$	$\hat{\theta}_{s9}$	$\hat{\theta}_{s10}$	$\hat{\theta}_{s11}$

The general structure of the five-level FLDTC for DSSM is represented by figure 5.

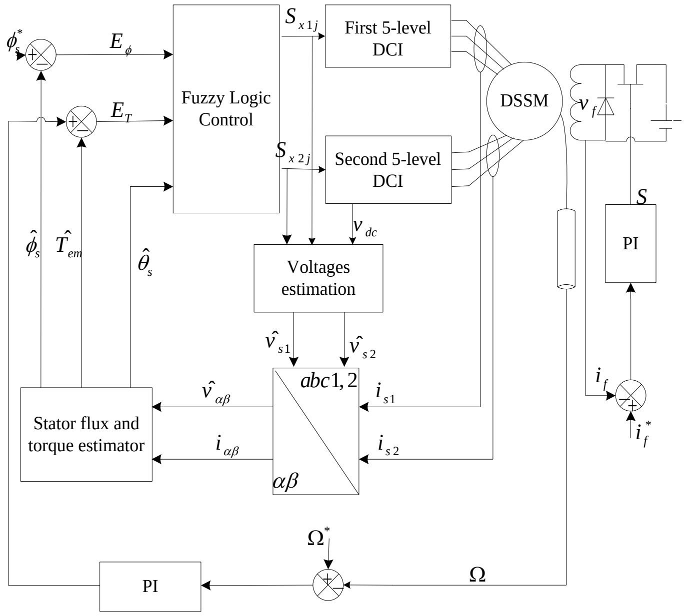

Fig. 5 Five-level FLDTC scheme for DSSM.

VI. Comparative Study

To verify the validity of the proposed controller, the system was simulated using the DSSM parameters given in Appendix. The DC side of the inverter is supplied by a constant DC source v_{dc}=*600*V. The aim of this section is to compare the five-level DTC for DSSM with the five-level FLDTC for DSSM.

The obtained results are presented in figure 6 for the five-level DTC and figure 7 for the five-level FLDTC. The DSSM is accelerate from standstill to reference speed *100* rad/s. the system simulated with load torque ($T_L = 11$ N.m), afterwards it is step variation on the rated load ($T_L = 0$ N.m) at time t=1s. And then a sudden reversion in the speed command from *100* rad/s to *-100* rad/s was introduced at *1.5*s.

In figure 6, the speed follows its reference value while the electromagnetic torque reaches slowly its reference value. Elimination of the load torque causes a slight variation in speed response. The speed controller intervenes to face this variation and ensures the system follows its suitable reference speed.

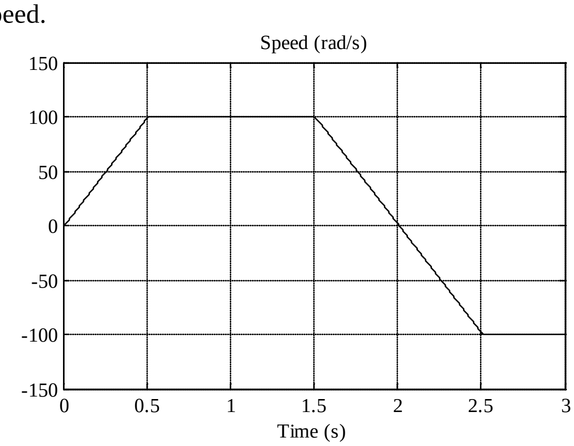

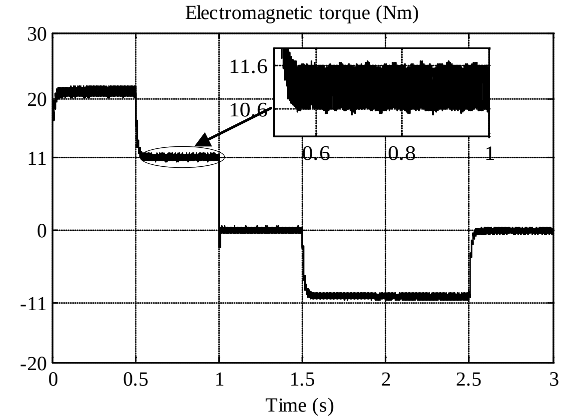

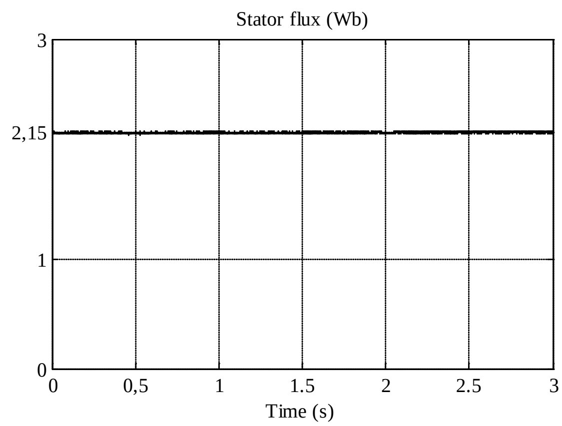

Fig. 6 Dynamic responses five-level DTC for DSSM.

Figure 7 illustrates that the system has a quick and smooth starting process and the command reject effectively the disturbance. The excellent dynamic performance of electromagnetic torque and flux control is evident. It must be pointed out that the five-level FLDTC decrease considerably the torque ripple.

The simulation results show that the five-level FLDTC is an effective solution for DSSM drives. In fact, this control ensures good decoupling between stator flux linkage and electromagnetic torque. Also, it can decrease the torque ripples in comparison to the five-level DTC with good dynamic performances.

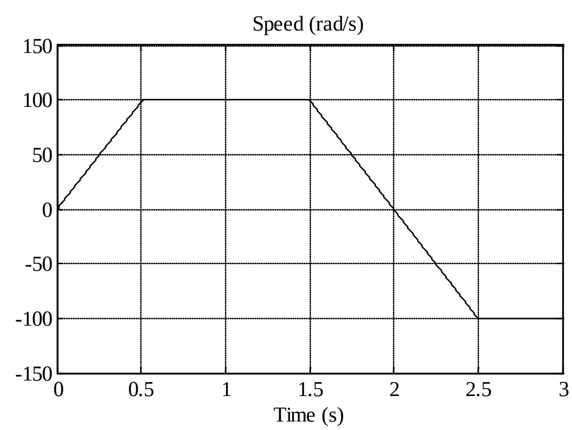

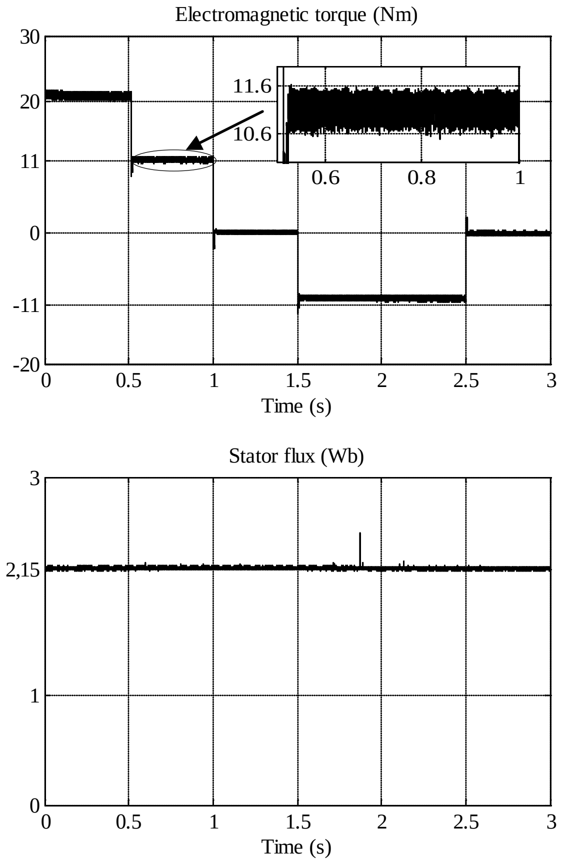

Fig. 7 Dynamic responses of five-level FLDTC for DSSM.

VII. Conclusion

In this paper, a multilevel DTC method applied on DSSM fed by two five-level inverters is presented and its merits over the conventional DTC approach are confirmed by simulation results.

Simulation results that have been presented in steady-state and transient operating conditions suggest that the proposed scheme is capable of giving satisfactory steady state and dynamic performance. Indeed, the drive operates with low ripple of motor variables and the decoupling between the stator flux and the electromagnetic torque is maintained, confirms the good performances of the developed drive systems. Moreover, by means the five-level inverter fed DTC drive, it is possible to reduce the stress of the switching devices of the voltage source inverter and lowering the switching power losses, often demanded requirements in high power applications.

VIII. Appendix: DSSM parameters

p_n=5 kW, v_n=232V, p=1, R=2.35 Ω, R_f=30.3Ω, L_d=0.3811H, L_q=0.211H, L_f=15H, M_{fd}=2.146H, J=0.05Nms^2/rad, f_r=0.001Nms/rad, i_f=1A.

IX. References

[1] B. Naas, L. Nezli, M. Mahmoudi, and M. Elbar, “Direct torque control based three-level inverter fed double star permanent magnet synchronous machine,” Energy Procedia, Vol. 18, 2012, pp. 521-530.

[2] K. Marouani, F. Khoucha, A. Khelouil, L. Baghli, and D. Hadiouche, “Study and simulation of direct torque control of double star induction motor drive,” IEEE, International Power Electronics and Motion Control Conference, May 2010, pp. 1233-1238.

[3] D. Boudana, L. Nezli, A. Tlemçani, and M. Mahmoudi, “DTC of double star synchronous machine drive using backstepping concept with fixed switching frequency,” International Symposium on Environment Friendly Energies in Electrical Applications, Algeria, 2010, pp. 1-6.

[4] P. Thongprasri, “A 5-level three-phase cascaded hybrid multilevel inverter,” International Journal of Computer and Electrical Engineering, Vol. 3, No. 6, 2011, pp. 789-794.

[5] B. Singh, N. Mittal, D. Verma, D. Singh, S. Singh, R. Dixit, M. Singh, and A. Baranwal, “Multi-level inverter: a literature survey on topologies and control strategies,” International Journal of Reviews in Computing, Vol. 10, 2012, pp. 1-16.

[6] C. Balamurugan, S. Natarajan, and R. Bensraj, “Investigations on three phase five-level diode clamped multilevel inverter,” International Journal of Modern Engineering Research, Vol. 2, No. 3, 2012, pp. 1273-1279.

[7] D. Boudana, L. Nezli, T. Mohand, O. Mahmoudi, and M. Tadjine, “Robust DTC based on adaptive fuzzy control of double star synchronous machine drive with fixed switching frequency, Journal of Electrical Engineering," Vol. 63, No. 3, 2012, pp. 133-143.

[8] B. Naas, A. Massoum, and B. Naas. “A Modified direct torque control six-sector of a double star permanent magnet synchronous machine based on fuzzy logic,” International Conference on Power Electronics and Electrical Drives, Oran, Algeria, December 2012.

[9] E. Benyoussef, A. Meroufel, and S. Barkat, “Direct torque control using fuzzy logic controller for double star synchronous machine,” International Conference on Power Electronics and Electrical Drives, Oran, Algeria, December 2012.

[10] W. Xuezh, and L. Huang, “Direct torque control of three-level inverter using neural networks as switching vector selector,” IEEE, Annual Meeting, 2001.

[11] R. Zaimmedine, E. Berkouk, and R. Duke, “A novel DTC scheme for a five-level voltage source inverter with GTO thyristors,” Third International Conference on Systems, Signals & Devices, 2005.

E. Benyoussef was born in M'sila (Algeria) in 1985. He received the Eng. Degree in Electrical Engineering from Mohammed Boudiaf University of M'sila in 2009 and the MS degree from the Electrical Engineering Institute of Sidi Bel Abbes University in 2011. He is a member of ICEPS (Intelligent Control Electrical Power System) Laboratory. His research interests are in modeling and robust control of dual three phase synchronous motors and converters.

A. Meroufel was born in Sidi Bel Abbes (Algeria) in 1954. He received his BS degree in electrical engineering from the UST Oran (Algeria) in 1980, the MS degree from the same University (USTO) in 1990 and the PhD degree from the Electrical Engineering Institute of University of Sidi Bel Abbes (Algeria) in 2004. He is currently Professor of electrical engineering in this University. He is a member of ICEPS (Intelligent Control Electrical Power System) Laboratory. His research interests are in robust control of electrical machines, Harmonics analysis methods and improvement of PFC, Non-linear control of electrical drives, Power electronics. He is an author and co-author of more than 30 scientific articles.

S. Barkat received his Engineer, Magister and Doctorate degrees, all in Electrical Engineering, from the Polytechnic National Institute of Algiers in 1994, 1997 and 2008 respectively. In 2000, he joined the Department of Electrical Engineering, University of M’sila. His current research interests are in the field of power electronics, renewable energies, multiphase drives, and advanced control theory and applications.